Cite this: *Chem. Commun.*, 2011, **47**, 9131–9133

www.rsc.org/chemcomm

COMMUNICATION

Deep ultraviolet tip-enhanced Raman scattering

Zhilin Yang,[a] Qianhong Li,[a] Yurui Fang[b] and Mengtao Sun*[b]

Received 3rd June 2011, Accepted 28th June 2011
DOI: 10.1039/c1cc13291a

Electromagnetic mechanism of deep ultraviolet tip-enhanced Raman scattering (DUV-TERS) is investigated theoretically with the finite-difference time-domain (FDTD) method, stimulated by recent DUV-TERS experimental reports. FDTD results reveal that the strongest electromagnetic enhancement factor for DUV-TERS is as high as 7 orders in the optimal geometry.

Tip-enhanced Raman scattering (TERS), which combines surface-enhanced Raman scattering (SERS) with scanning probe microscopy (SPM), such as scanning tunneling microscopy (STM), atomic force microscopy (AFM), or scanning near field optical microscopy (SNOM), provides not only rich spectral and structural information of tiny amounts of the probe molecules even down to a single-molecule level near the metal tip but also a high spatial resolution of the sample simultaneously.[1–5]

The investigation of the deep ultraviolet SERS (DUV-SERS) and the deep ultraviolet tip enhanced Raman scattering (DUV-TERS) is rapidly evolving, because of their advantages and application in bioscience and material sciences.[6–18] In the search for DUV-TERS material, aluminium (Al) is found to be one of the best candidates, because it has low absorption down to a wavelength of 200 nm due to its free-electron-like character and plasmon resonance in the UV range. In the DUV region, the dielectric function of aluminium shows reasonably small imaginary part, whereas the real part keeps negative. Hence, it is reasonable to expect that aluminium is one of the most promising plasmonic materials for achieving surface plasmon enhancement in the DUV region.[19] Experimentally, Taguchi *et al.*, for the first time, reported the DUV-TERRS (tip-enhanced resonance Raman scattering), where the substrate and the tip are the Al film and the Al coated on the silicon tip, respectively.[12]

Based on Taguchi's experimental report,[12] and our previous theoretical study on TERS in the visual region,[20,21] DUV-SERS on Al nanoparticles[6] and DUV-nanoholes on an Al film,[22] we theoretical investigate the electromagnetic mechanism of DUV-TERS in this work, in order to find optimal geometric parameters of the tip and the substrate with side illumination, using the finite-difference time-domain (FDTD) method.[23] The model in the calculations can be seen from Fig. 1(a). The optical constant data are taken from experimental results from ref. 24. A nonuniform Mesh method was adopted to save simulation time. Mesh accuracy was set at 5 for the overall simulation region and smaller mesh was chosen around the tip.

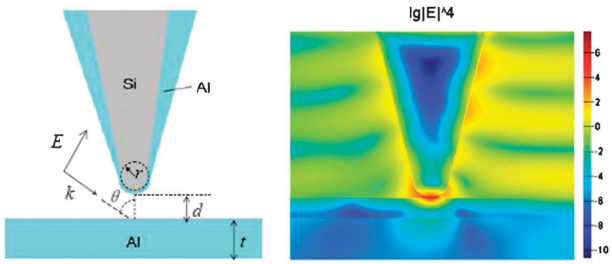

Fig. 1 (a) The model of DUV-TERS in the calculations, and (b) the near field distribution of DUV-TERS excited at 233 nm, where $\theta = 25^\circ$, $d = 2$ nm, $t = 40$ nm, $r = 15$ nm for silicon, thickness of Al on the silicon tip is 15 nm.

As a reference, we firstly study the DUV-TERS, where the tip is pure Al. Fig. 2(a) shows incident angle (θ) dependent DUV-TERS enhancement, where the thickness of the Al substrate is $t = 40$ nm, the tip is modeled as a conical taper terminated by a hemisphere of radius $r = 30$ nm, and the gap between the tip and the surface is $d = 2$ nm. The strongest

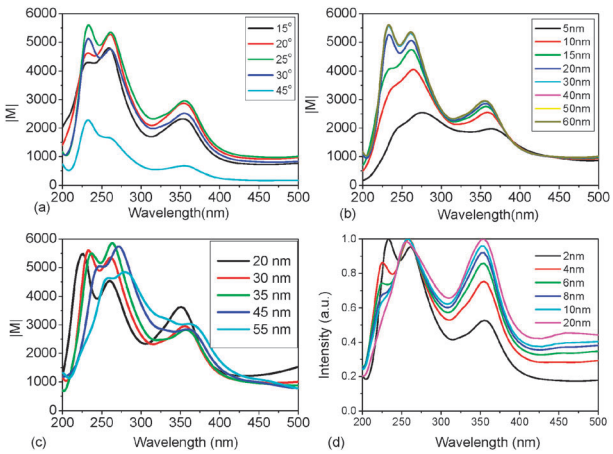

Fig. 2 (a) The incident angle, (b) the thickness of the substrate, (c) the hemisphere radius, and (d) the distance dependent surface plasmon enhancements of DUV-TERS, where $|M| = |E_{local}/E_{in}|$, and E_{local} and E_{in} are local and incident electric fields, respectively.

[a] *Department of physics, Xiamen University, Xiamen, 361005, P. R. China*
[b] *Beijing National Laboratory for Condensed Matter Physics, Institute of Physics, Chinese Academy of Sciences, P. O. Box 603-146, Beijing, 100190, P. R. China. E-mail: mtsun@aphy.iphy.ac.cn*

electromagnetic field enhancement at the center of the nanogap between the tip and the substrate is considered in the calculations. Fig. 2(a) shows that the strong electromagnetic enhancement will occur in the range from 200 nm to 400 nm, and there are three peaks around 233, 261 and 365 nm; furthermore, the strongest surface plasmons are in the region of 200 nm to 300 nm. It is found that when θ is set to 25°, the strongest local electromagnetic enhancement can be obtained, which is significantly different from the Au TERS system (where the tip and the substrate are all made from Au), in which the best θ is 60° for the Au TERS system at the incident light of 632.8 nm.[20,21] The parameters in the calculations of Fig. 2(a) are reasonable, which can be confirmed by below calculations.

Fig. 2(b) shows that the electromagnetic enhancement will increase sharply and blue shift, when the thickness of the Al substrate t increases from 5 to 15 nm; while from 20 to 30 nm, electromagnetic enhancement will increase gradually. When t is larger than 30 nm, the electromagnetic enhancement will be stable and will not increase. It is understandable that these peaks in Fig. 2(b) will increase with t from 5 nm to 30 nm. If the substrate is too thin, it cannot localize in the nanogap between the tip and the substrate well, and will penetrate into the substrate, due to the decay depth ($I/I_0 = 1/e$) perpendicular to the substrate.

Fig. 2(c) reveals that the optimal hemisphere radius should be 20 nm $< r <$ 45 nm, and when $r >$ 45 nm, the electromagnetic field enhancement will decrease. It is known that the electromagnetic field enhancement in the nanogap between the tip and the surface results from the balance between the lightning-rod effect and size effect of the tip. It is found that these three peaks will be red shifted with the increase of r. The distance between the tip and the substrate is $d = 2$ nm in the calculations shown in Fig. 2(a), which is also reasonable. Our theoretical studies reveal that when $d \leq 2$ nm, the hot site is localized at the center between the tip and the substrate, when $d \geq 4$ nm, the hot site is at 1 nm below the tip, and when the $d < 1$ nm, the calculated result is not reasonable, due to electron tunneling transfer between the tip and the substrate. Fig. 2(d) shows change in electromagnetic field enhancement with the distance between the tip and the substrate. Note that the intensities are normalized to 1 for comparison. It is found that peaks at 258 and 354 nm will not shift with the increase of the distance from 2 nm to 10 nm, while the peak at 232 nm ($d = 2$ nm) will be blue shifted slightly; further more when $d = 20$ nm, this peak disappeared. So, the peak at 232 nm should result from the strong coupling between the tip and the substrate, and the other two peaks should originally result from the tip, and should be enhanced by the coupling between the tip and the surface; furthermore, these two peaks are almost not shifted with the change in distance between the tip and the surface. Note that the change in distance can only influence the intensity of the other two peaks by coupling effect between the tip and the surface, but these two peaks are not shifted.

Now, we study the electromagnetic field enhancement of DUV-TERS, where the silicon tip is coated by Al with different thickness. When $t = 40$ nm, $d = 2$ nm and $r = 15$ nm, we study electromagnetic enhancement in the nanogap, where different

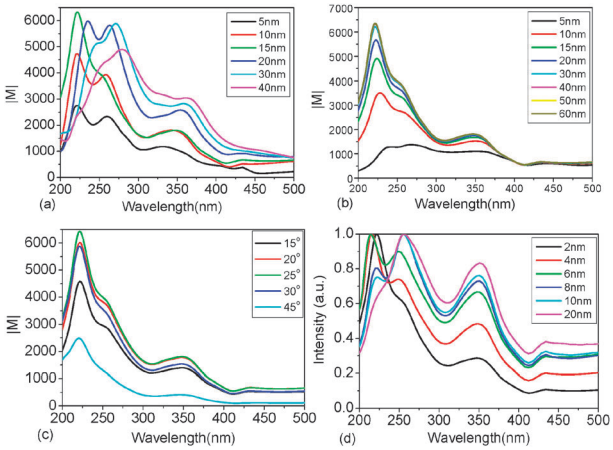

Fig. 3 (a) The hemisphere radius, (b) the thickness of the substrate, (c) the incident angle, and (d) the distance dependent surface plasmon enhancements of DUV-TERS, where the tip is an Al coated silicon tip.

thickness of coated Al (shell) is considered (see Fig. 3(a)). It is found that with the increase of thickness of coated Al from 5 to 15 nm, the intensities of the electromagnetic field at 222 and 260 nm will sharply increase. When the thickness of coated Al is larger than 15 nm, these two peaks will be red shifted. If the thickness of coated Al is large enough (>40 nm), the intensity of these peaks will decrease gradually. So, it is better that the thickness of coated Al on the silicon tip is between 15 nm and 30 nm. When the thickness of coated Al on the silicon tip is larger than 15 nm, the changing tendency of both position and intensities of peaks is similar to the case of pure Al tip shown in Fig. 2(c). Fig 3(b) reveals that the intensities of electromagnetic field enhancement are sharply increased with the increase of thickness of the substrate. When $t >$ 30 nm, the electromagnetic field enhancement will not increase too much. This qualitative conclusion is similar to those in Fig. 2(b). To check whether $\theta = 25°$ is the best one, we studied θ dependent electromagnetic field enhancement (see Fig. 3(c)), where $t = 40$ nm, and the thickness of coated Al on the silicon tip is 15 nm in the calculations. Fig. 3(c) reveals that when θ ranges from 15° to 25°, the intensity of the peak at 222 nm is increased; when $\theta > 25°$, the intensity of the peak at 222 nm is decreased. So, $\theta = 25°$ is the best one, which is similar to the case shown in Fig. 2(a). Fig. 3(d) shows the distance dependent electromagnetic enhancement. Note that the intensities are normalized to 1 for comparison. It is found that the peak at 222 nm will decrease with the increase of distance, and will disappear when the distance is 20 nm. So, this peak is totally dependent on the coupling between the tip and the substrate. The other two peaks originally should result from the tip, and should be enhanced by the coupling between the tip and the surface; furthermore, these two peaks are almost not shifted with the change in the distance between the tip and the substrate. Fig. 1(b) is the near field distribution in the DUV-TERS system with optimal parameters, where $t = 40$ nm, $d = 2$ nm, the hemisphere radius of silicon (core) $r = 15$ nm, the thickness of the coated Al on the silicon tip is 15 nm, the incident angle is 25°, and the incident light is 222 nm. It is found that the strongest electromagnetic enhancements

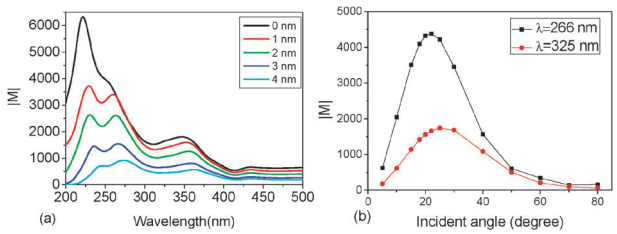

Fig. 4 (a) The thickness of the Al_2O_3 layer dependent electromagnetic field at $\theta = 25°$, where the thickness of Al coated on the silicon tip is 15 nm, $t = 40$ nm, where the thickness of Al_2O_3 is included in the thickness of Al. (b) Electromagnetic enhancement of DUV-TERS, where $d = 2$ nm, $t = 40$ nm, $r = 15$ nm for silicon, the thickness of Al on the silicon tip is 15 nm.

are localized in the center of the nanogap between the tip and the substrate.

It is noted that the surfaces of the Al tip and substrates are easily oxidized, and the thickness of Al_2O_3 is often 1 to 2 nm. Fig. 4(a) reveals that the intensities of electromagnetic field enhancements will decrease slightly with the increase of thickness of Al_2O_3. It is tolerable to measure DUV-TERS spectra, since the maximum SERS enhancement shows about one order of magnitude decrease when a 2 nm Al_2O_3 layer forms on the pure Al surface. This Al_2O_3 layer is particularly useful sometimes because a natural born oxide layer provides an isolated layer to prevent the direct interaction between Al and the probe molecules, similar to that of shell-isolated nanoparticle enhanced Raman spectroscopy (SHINERS).[22,25] Also, when the waist of the Gaussian beam is fixed for the width wavelength from 200 to 500 nm in the calculations, the accurate incident angle should be fixed at 350 nm, and the incident angles will be slightly changed with the changes in wavelength. To obtain accurate optimal incident light at 266 and 325 nm, respectively, we further calculated incident angle dependent electromagnetic enhancement, which can be seen from Fig. 4(b). It is found that the optimal incident angles at 325 and 266 nm are 25°, and 22°, respectively.

In conclusion, electromagnetic mechanism of DUV-TERS has been investigated theoretically, using the FDTD method. The FDTD results revealed that the conditions of the strongest local plasmon are $\theta = 22°$, $t > 40$ nm, and the thickness of silicon coated on the Al tip is from 15 nm to 30 nm. There is not too much influence of the Al_2O_3 layer on DUV-TERS to obtain DUV-TERS signals. Our results offer abundant opportunities to understand the underlying mechanism of DUV-TERS and design a high efficiency platform for DUV-TERS studies and applications.

This work was supported by the National Natural Science Foundation of China (Grant Nos 11074210, 10874234, 90923003 and 20703064), the National Basic Research Project of China (Grant Nos 2009CB930701, 2009CB930703 and 2007CB936804).

Notes and references

1 A. Hartschuh, E. J. Sanchez, X. S. Xie and L. Novotny, *Phys. Rev. Lett.*, 2003, **90**, 095503.
2 K. F. Domke, D. Zhang and B. Pettinger, *J. Am. Chem. Soc.*, 2006, **128**, 14721.
3 E. Bailo and V. Deckert, *Chem. Soc. Rev.*, 2008, **37**, 921.
4 B. Ren, G. Picardi, B. Pettinger, R. Schuster and G. Ertl, *Angew. Chem., Int. Ed.*, 2005, **44**, 139.
5 J. Steidtner and B. Pettinger, *Phys. Rev. Lett.*, 2008, **100**, 236101.
6 M. T. Sun, S. Zhang, Y. Fang, Z. Yang, D. Wu, B. Dong and H. X. Xu, *J. Phys. Chem. C*, 2009, **113**, 19328.
7 S. A. Asher, *Anal. Chem.*, 1993, **65**, 59A; S. A. Asher, *Anal. Chem.*, 1993, **65**, 201A.
8 S. P. A. Fodor and T. G. Spiro, *J. Am. Chem. Soc.*, 1986, **108**, 3198.
9 X. F. Lin, B. Ren, Z. L. Yang, G. K. Liu and Z. Q. Tian, *J. Raman Spectrosc.*, 2005, **36**, 606.
10 B. Ren, X. F. Lin, Z. L. Yang, G. K. Liu, R. F. Aroca, B. W. Mao and Z. Q. Tian, *J. Am. Chem. Soc.*, 2003, **125**, 9598.
11 L. Hecht, J. Clarkson, B. J. E. Smith and R. Springett, *J. Raman Spectrosc.*, 2007, **37**, 562.
12 A. Taguchi, N. Hayazawa, K. Furusawa, H. Ishitobi and S. Kawata, *J. Raman Spectrosc.*, 2009, **40**, 1324.
13 S. O. Konorov, H. Schulze, C. J. Addison, C. A. Haynes, M. W. Blades and R. F. B. Turner, *J. Raman Spectrosc.*, 2009, **40**, 1162.
14 H. S. Shafaat, K. M. Sanchez, T. J. Neary and J. E. Kim, *J. Raman Spectrosc.*, 2009, **40**, 1060.
15 A. Fujiwara and Y. Mizutani, *J. Raman Spectrosc.*, 2008, **39**, 1600.
16 C. Huang, G. Balakrishnan and T. G. Spiro, *J. Raman Spectrosc.*, 2006, **37**, 277.
17 V. Shashilov and I. K. Lednev, *J. Am. Chem. Soc.*, 2008, **130**, 309.
18 T. Dorfer, M. Schmitt and J. Popp, *J. Raman Spectrosc.*, 2007, **38**, 1379.
19 Y. Watanabe, W. Inami and Y. Kawata, *J. Appl. Phys.*, 2011, **109**, 023112.
20 Z. Yang, J. Aizpuruac and H. X. Xu, *J. Raman Spectrosc.*, 2009, **40**, 1343.
21 M. T. Sun, Y. R. Fang, Z. L. Yang and H. X. Xu, *Phys. Chem. Chem. Phys.*, 2009, **11**, 9421.
22 Z. L. Yang, Q. H. Li, B. Ren and Z. Q. Tian, *Chem. Commun.*, 2011, **47**, 3909.
23 K. S. Kunz and R. J. Luebber, *The Finite Difference Time Domain Method for Electromagnetics*, CRC, Cleveland, 1993.
24 O. J. F. Martin and C. Girard, *Appl. Phys. Lett.*, 1997, **70**, 10.
25 J. F. Li, Y. Ding, Y. F. Huang, Z. L. Yang, S. B. Li, X. S. Zhou, F. R. Fan, W. Zhang, Z. Y. Zhou, D. Y. Wu, B. Ren, Z. L. Wang and Z. Q. Tian, *Nature*, 2010, **464**, 392.